A potential vorticity view of synoptic development

Brian Hoskins, *Department of Meteorology, University of Reading, PO Box 243, Reading RG6 6BB, UK*

A physical discussion of vorticity and its change by stretching and tilting is presented. The discussion naturally leads on to the conservation of quasi-geostrophic potential vorticity, q, and the flow associated with anomalies in q. The extension to full potential vorticity (PV) and the associated conservation and inversion properties is made. The use for illustrating and understanding synoptic developments of maps of PV on isentropic surfaces and potential temperature (θ) on PV surfaces is shown by considering two recent examples in the North Atlantic–Europe regions. The first is a summer situation and the second is the major blocking in January 1996. Concluding comments about the role of diabatic processes and other possible uses of these diagnostics are made.

1. Introduction

In this paper, a physical discussion of vorticity and potential vorticity (PV) is presented, with a minimum of mathematical equations, these being given in an Appendix. The application of PV thinking to viewing and understanding the development of mid-latitude weather systems will then be briefly discussed. A more theoretical and complete discussion of PV may be found in Hoskins *et al.* (1985). Synoptic applications are given in Hoskins & Berrisford (1988) and numerous recent papers.

2. Vorticity

Vorticity is a measure of the local rotation or spin in the atmosphere. As illustrated in Figure 1, the vector vorticity gives the direction of the axis of the spin and its magnitude is twice the local angular velocity about this axis. The relationship between the absolute vorticity, ζ, and the relative vorticity, ξ, may be written:

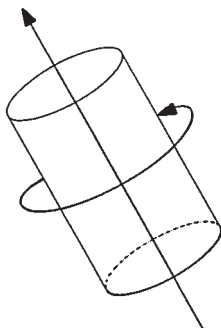$$\tfrac{1}{2}\zeta = \tfrac{1}{2}\xi + \Omega$$

Figure 1. *A vorticity vector and the local rotation in the atmosphere indicated by the circulation around a cylinder of air oriented along the vorticity vector.*

This says that the absolute spin is equal to the relative spin plus the rotation of the co-ordinate system, Ω.

In horizontal flow with the velocity described by a streamfunction ψ, the vertical component of relative vorticity is $\xi = \nabla^2\psi$. Thus if ξ is known everywhere and we have suitable boundary conditions, we can invert (i.e. solve the equation) to get ψ, and hence the velocity field, everywhere.

The vorticity equation (equation (A7)) has two generation terms. The second of these can be simply described as a horizontal vorticity tendency in the sense of warm air rising and cold air descending. The effect of the first term may be intuitively understood through the sketches in Figure 2. If the motion is such as to stretch the vorticity vector (Figure 2(*a*)), then the spin, and thus the magnitude of the vorticity, is increased (Figure 2(*b*)). If the motion is such as to tilt the vorticity vector (Figure 2(*c*)), then the direction of the spin and the vorticity vector is tilted (Figure 2(*d*)). These effects are known as vortex stretching and tilting (or twisting).

3. Quasi-geostrophic (QG) theory

In quasi-geostrophic (QG) theory only the vertical component of the vorticity equation (equation (A8)) is explicitly considered. It is also supposed that the Earth's rotation dominates: $\zeta \cong f$. The relevant vorticity equation (equation (A15)) then contains only stretching and shrinking of this basic rotation. Two simple examples are shown in Figure 3. Along with zero vertical motion at the ground, mid-tropospheric ascent implies stretching and the creation of absolute vorticity greater than f, i.e. cyclonic relative vorticity, in the lower troposphere. Similarly mid-tropospheric descent implies shrinking and creation of relative anticyclonic vorticity.
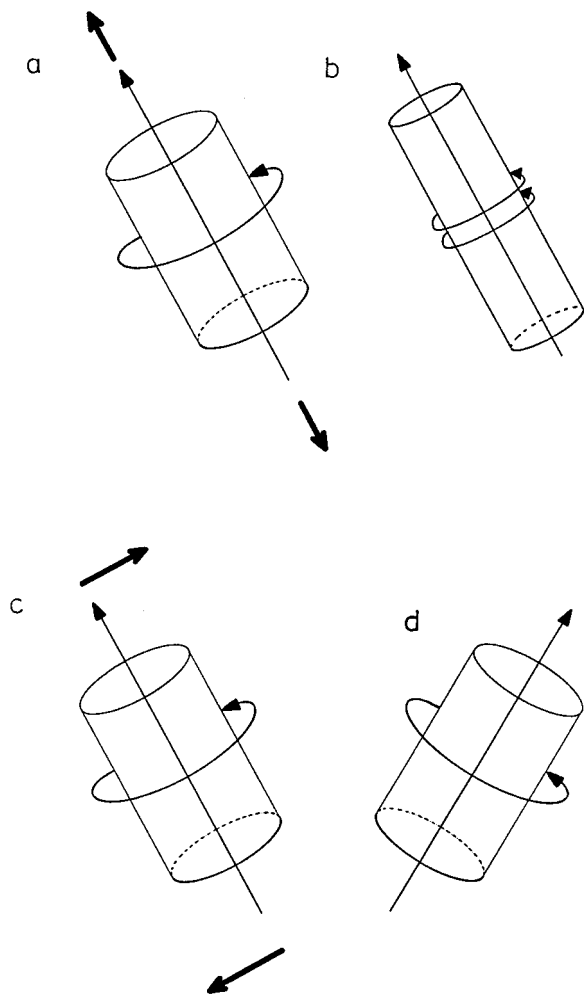
Figure 2. *The change in vorticity associated with the stretching and tilting of the vorticity vector. The tendency of the motion to stretch the vorticity in (a) leads to greater circulation around a taller, thinner cylinder and larger vorticity shown in (b). The tendency of the motion to tilt the vorticity in (c) leads to the same circulation around a tilted cylinder and tilted vorticity shown in (d).*

Consistent with this discussion, synoptic development can be viewed in terms of the vertical velocity derived from the so-called QG omega equation (equation (A20) with equations (A21), (A22) or (A24)), and the predictive vorticity equation (equation (A15)). This approach is discussed in Pedder (1997).

An alternative but equivalent approach is to note that the amount of stretching that has taken place is indicated by the distortion of potential temperature contours, as in Figure 4. This in turn is described by the thermodynamic energy equation (equation (A16)). Combining this equation with the vorticity equation (equation (A15)) gives the conservation equation (equation (A17)) for QG potential vorticity q (equations (A18) and (A19)). For a uniform static stability, resting basic state and constant f, then $q = f$. At a later time:

$$q = f + \xi + f \frac{\partial \theta'}{\partial z} / \frac{d\bar{\theta}}{dz}$$
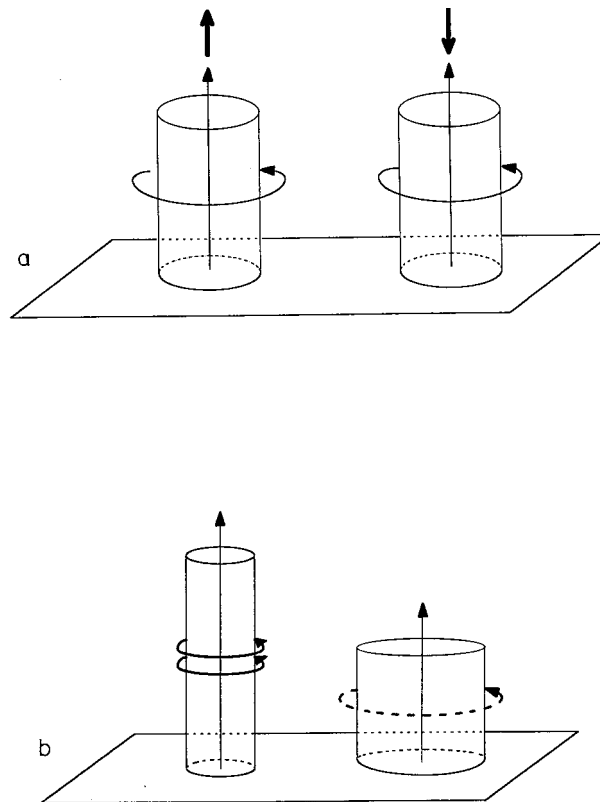

Figure 3. *Mid-tropospheric ascent and descent shown in (a) leads to, respectively, the stretching and shrinking of vorticity and the associated increase and decrease of vorticity and circulation shown in (b). If the initial relative vorticity is zero, the two situations correspond to cyclonic and anticyclonic surface developments.*

where $\bar{\theta}(z)$ is a reference potential temperature and θ' the departure from this.

The conservation of q then gives:

reduced static stability

$$\Rightarrow \frac{\partial \theta'}{\partial z} < 0 \quad \Rightarrow \xi > 0, \text{ cyclonic,}$$

increased static stability

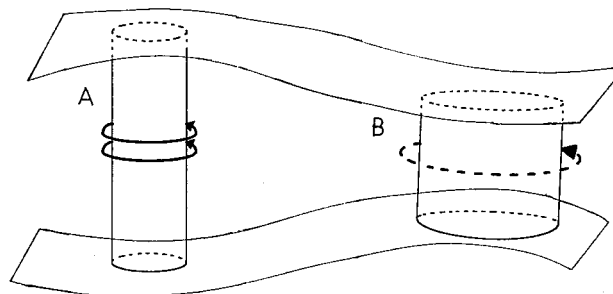$$\Rightarrow \frac{\partial \theta'}{\partial z} > 0 \quad \Rightarrow \xi < 0, \text{ anticyclonic,}$$

Figure 4. *The stretching and shrinking of the two cylinders bounded by the two isentropic (potential temperature) surfaces, and hence the change in vorticity and circulation, in going from A to B, or vice versa, is indicated by the relative separation of these two surfaces.*
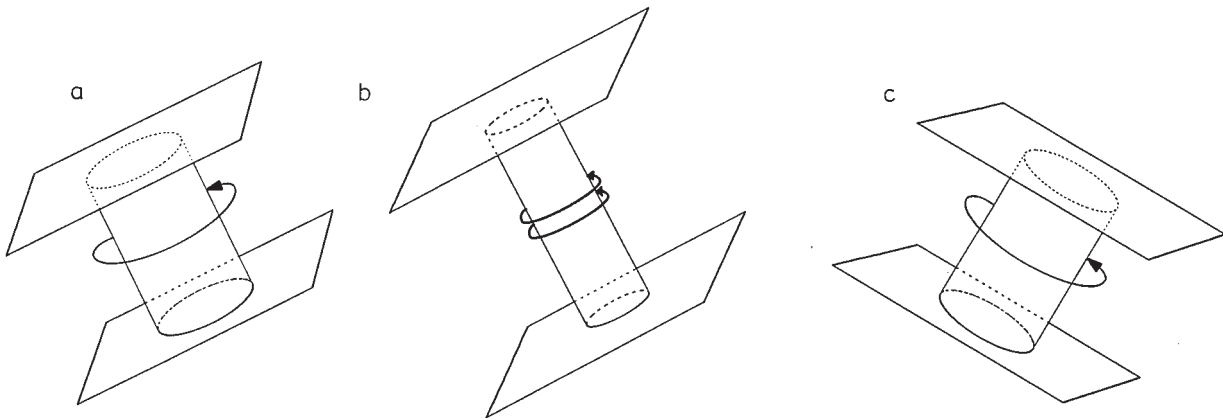
Figure 5. *The cylinder between two isentropic surfaces in (a) is stretched in (b) and tilted in (c). The vorticity normal to the isentropic surface is increased in (b) and tilted with the cylinder in (c).*

consistent with points A and B, respectively, in Figure 4.

The form of the equation for q in terms of the QG streamfunction (equation (A19)) shows that, given q everywhere and suitable boundary conditions, the equation can be inverted to give ψ and hence ϕ, $\mathbf{v}_g$ and θ everywhere. This is analogous to the inversion of the vorticity in the two-dimensional case (see section 2).

4. Full (Rossby–Ertel) potential vorticity

The same ideas can be used without making the QG approximations. Consider a thin cylinder between two neighbouring isentropic surfaces, Δh apart (Figure 5(a)). The quantity:

$$P = \zeta_n / \rho \Delta h$$

is conserved where $\frac{1}{2}\zeta_n$ is the spin of the cylinder. This takes account of stretching: Δh and ζ_n both increase or both decrease (Figure 5(b)). It takes account of tilting because the cylinder tilts with the fluid (Figure 5(c)). It also takes account of density changes which have been neglected elsewhere in this discussion for simplicity.

Since $|\nabla\theta| = \Delta\theta/\Delta h$ and $\Delta\theta$ (the difference in potential temperature between the two isentropic surfaces) is constant following the motion, then the conservation of P is equivalent to the conservation of:

$$P = \Delta\theta\, P = \frac{1}{\rho}\zeta_n\, |\nabla\theta|$$

where P is the so-called potential vorticity (PV). It is equivalent to the form given in equation (A27). Thus it is seen that the adiabatic, frictionless conservation of PV (equation (A28)) is simply related to conservation of P and to the ideas discussed above. The mathematical relationship of QGPV conservation to full PV conservation is not immediate but the physical relationship is clear.

PV has two basic properties:

(a) Conservation. If the motion is adiabatic and frictionless then PV is conserved moving with the air.
(b) Inversion. Given PV everywhere and suitable boundary conditions, and assuming that the motion is balanced in the sense that it is not composed of fast gravity waves (or acoustic waves), then equations can be solved to obtain ϕ, $\mathbf{v}$, θ, w, etc. This is analogous to the two-dimensional and QGPV cases discussed above.

We can now think about the PV distribution itself rather than the behaviour of cylinders between isentropic surfaces, but the results must be the same. Figure 6(a) indicates the situation usually associated with a positive PV anomaly, i.e. a region in which the PV is larger than in the surrounding air. Inside the region the vorticity and static stability ($\propto 1/\Delta h$) are both large.
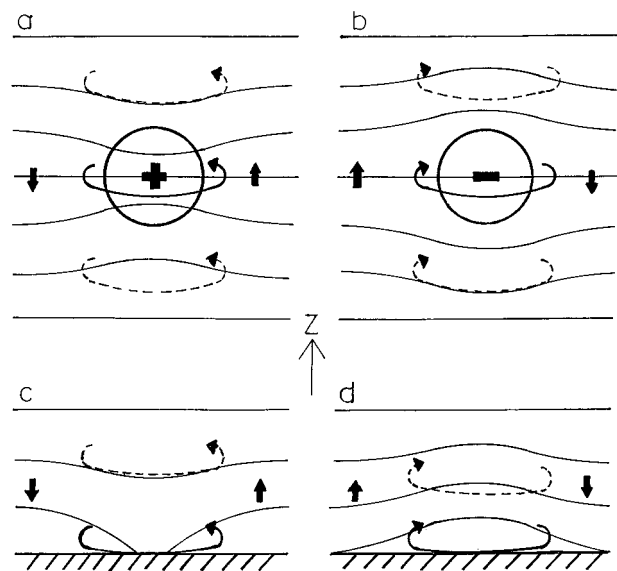

Figure 6. *The isentropes and circulation for idealised positive (a) and negative (b) interior PV anomalies, and for warm (c) and cold (d) surface temperature anomalies. Also shown is the sense of the vertical motion if there is a basic flow along the sections which increases with height. (Adapted from Hoskins, et al., 1985; Thorpe, 1985; Hoskins & Berrisford, 1988.)*
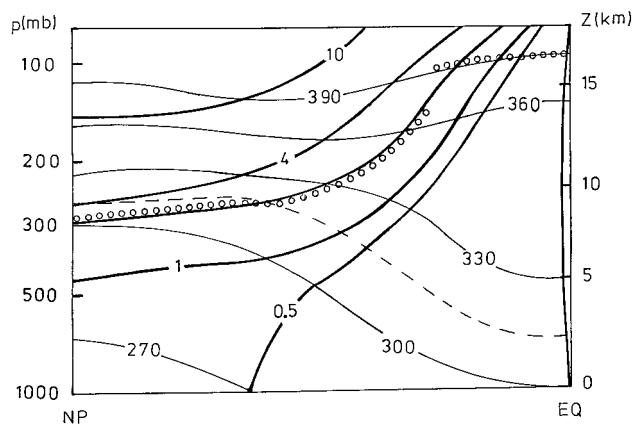
327

Figure 7. *A schematic latitude–height section from north pole to equator showing isentropes, PV contours and the tropopause. The isentropes are drawn lightly every 30 K starting at 270 K, but with the 315 K surface indicated by dashes. The PV contours are drawn in bold at 0.5, 1, 2, 4, 10 PVU, where 1 PVU = 10^{-6} m^2 K s^{-1} kg^{-1}. The tropopause is indicated by a line of open circles. (Adapted from Hoskins, 1991.)*

Outside the anomaly, but close to it, the isentropes must be separated more than they would be if the anomaly was not present and the vorticity must be greater than f (i.e. cyclonic). It can also be shown that if there is a 'zonal' wind increasing with height there will be ascent to the 'east' of the anomaly and descent to the 'west'. Thus the influence of the anomaly is apparent in the surrounding air. Figure 6(*b*) shows a similar but negative, anticyclonic PV anomaly.

For a uniform PV fluid near a lower boundary with a warm anomaly (Figure 6(*c*)) the isentropic separation is enhanced and this must be associated with cyclonic

motion. Similarly, a cold lower boundary anomaly is associated with anticyclonic motion (Figure 6(*d*)).

Figure 7 shows a schematic latitude–height distribution of two variables θ and PV that are materially conserved in adiabatic, frictionless motion. An isentropic surface such as that at θ = 315 K slopes upwards from the lower troposphere in the tropics to the tropopause in middle latitudes and then levels off in the stratosphere. PV is measured in PVU where 1 PVU equals 10^{-6} m^2 K s^{-1} kg^{-1}. It increases polewards and upwards. Looking from the subtropical jet to the pole, there is a jump in PV values typically from 1.5 to 4 PVU at the tropopause and then a rapid increase with height in the stratosphere.

In an adiabatic, frictionless atmosphere PV contours will be advected on any θ-surface. On a θ-surface crossing the tropopause (e.g. Figure 8(c) below) contours in the range 2–3 may be considered as marking the boundary between low PV, lower latitude tropospheric air and high PV, higher latitude stratospheric air.

It is also clear that θ contours will be advected on a PV surface. A surface at values like PV = 2–3 is particularly useful because this can be considered to be a dynamical tropopause poleward of the subtropical jet (e.g. Figure 8(*d*) below). On such a map, higher latitude air has relatively low θ and lower latitude air has relatively high θ. (Note that on the tropopause the latitudinal gradient of θ is the reverse of that of T.)

Close to the equator PV values are small and do not usefully define a tropopause. For the southern hemi-
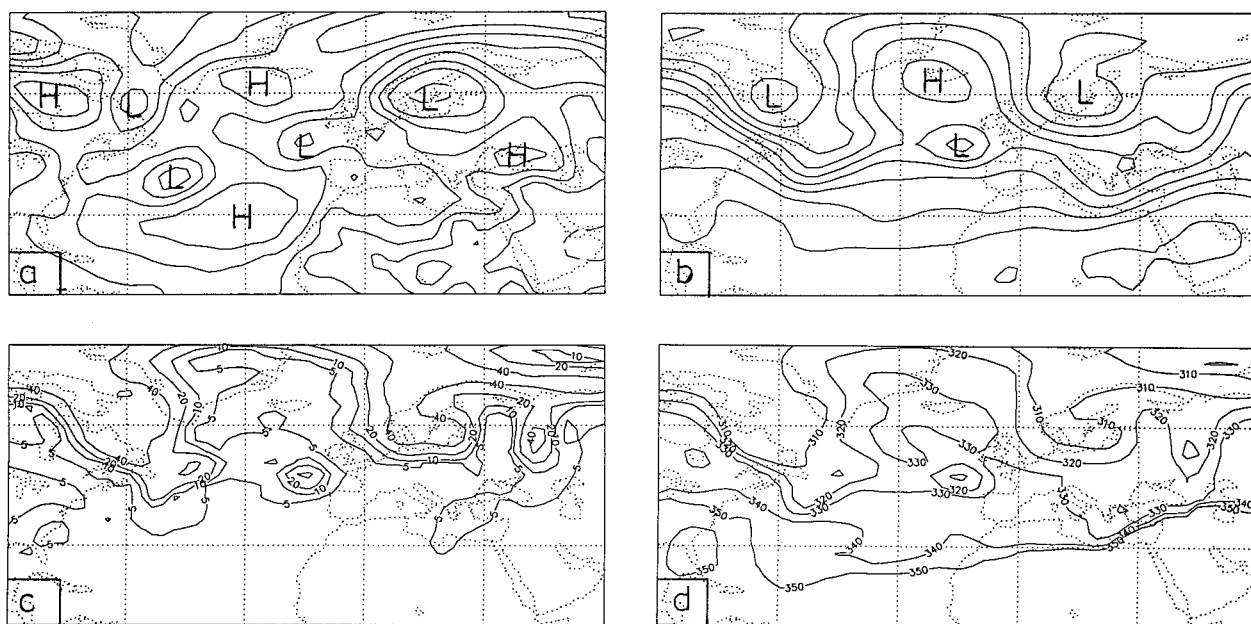

Figure 8. *Maps derived from ECMWF data for 1200 Z on 19 June 1996 (a) 1000 mb height, (b) 250 mb height, (c) PV on the 315 K isentropic surface, (d) potential temperature on the PV = 2 surface. The region shown is 90° W–60° E, 10° N–80° N with lines of longitude every 30° and lines of latitude at 30° N and 60° N indicated. The contour intervals are 30 m and 100 m in (a) and (b) respectively. The contours in (c) are drawn at 0.5, 1, 2, 4, and 8 PVU and marked by 10 times these values. The contours in (d) are drawn every 10 K up to 350 K but suppressed beyond this because the PV surface becomes vertical near the equator.*

sphere the above discussion applies with the same PV magnitudes but reversed signs.

5. Two examples

In this section PV maps will be shown for two recent sequences of weather, concentrating on the sector including the UK. Figures 8(*a*) and 8(*b*) show the 1000 mb and 250 mb height fields for 1200 Z on 19 June 1996. The UK was influenced by the northerly flow associated with a low centred over Scandinavia and also by a trough associated with a cut-off to the southwest. Figures 8(*c*) and 8(*d*) show the 315 K PV and the 2 PVU θ maps for this time. Both of these show the general relationship of height field troughs and cut-off lows with higher latitude air as indicated by relatively high PV or low tropopause θ, and height field ridges and cut-off highs with lower latitude air with relatively low PV or high tropopause θ. (Note that, if it was drawn in Figure 8(*d*), the 315K contour would be identical to the PV = 2 contour in Figure 8(*c*).)

The height field maps are often viewed as heavily smoothed versions of the PV or θ contour maps. On the latter, as long as the adiabatic assumption is valid, features are advected with their magnitudes conserved whereas features on the geopotential maps have no such property. We can, for example, look at the origin of the two high PV features influencing the UK on 19 June.

The sequence of daily 315 K PV maps for the period 14–19 June is shown in Figure 9. There are many features of interest in these. However, here we concentrate on a particular feature. The tip of the PV 'trough' (high, cyclonic PV) south of Greenland on 14 June cuts off by 15 June. This cut-off moves only slowly over the next few days. A further cut-off from the trough is evident (over Iceland) by 16 June. This second cut-off moves southeast into Europe while the first cut-off moves towards the southwest UK by 19 June. There is a clear picture of the UK being originally dominated by anticyclonic low PV and then influenced by two features originating from the same North Atlantic trough but approaching from different directions.

The winter 1995–96 was one of strong blocking in the Northwest European region. The Scandinavian blocking anticyclonic signature is evident in the average 250 mb and 1000 mb heights for the second half of January 1996, as shown in Figure 10. A 16 day sequence of 315 K PV maps in this period is given in Figure 11. It is clear that a succession of PV 'ridges' and 'troughs' develop in the baroclinic flow over North America and amplify over the North Atlantic. As they reach a stagnation point in the upstream side of the block, they break, with anticyclonic, low PV cut-offs to the north and cyclonic, high PV cut-offs to the south. These act to invigorate the blocking anticyclonic–cyclonic dipole. The high PV anomalies tend to all decay *in situ*, whereas a portion of the low PV anomaly air appears to
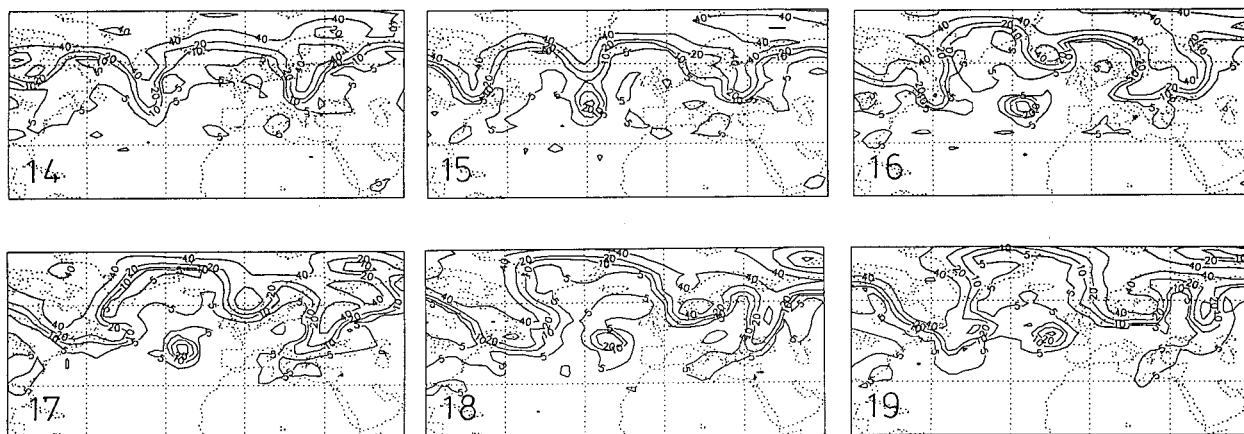

Figure 9. *315 K PV maps for 14–19 June 1996. The conventions are as in Figure 8(*c*)*
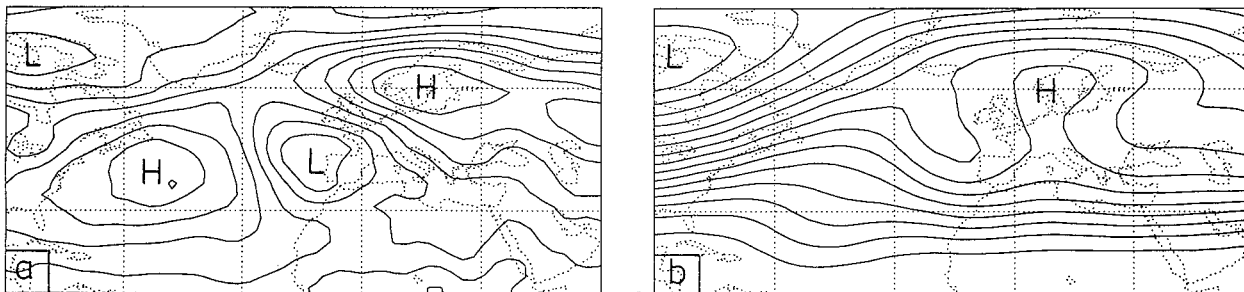

Figure 10. (a) *1000 mb and* (b) *250 mb average height fields for 16–31 January 1996. The conventions are as in Figures 8(*a*) and 8(*b*).*
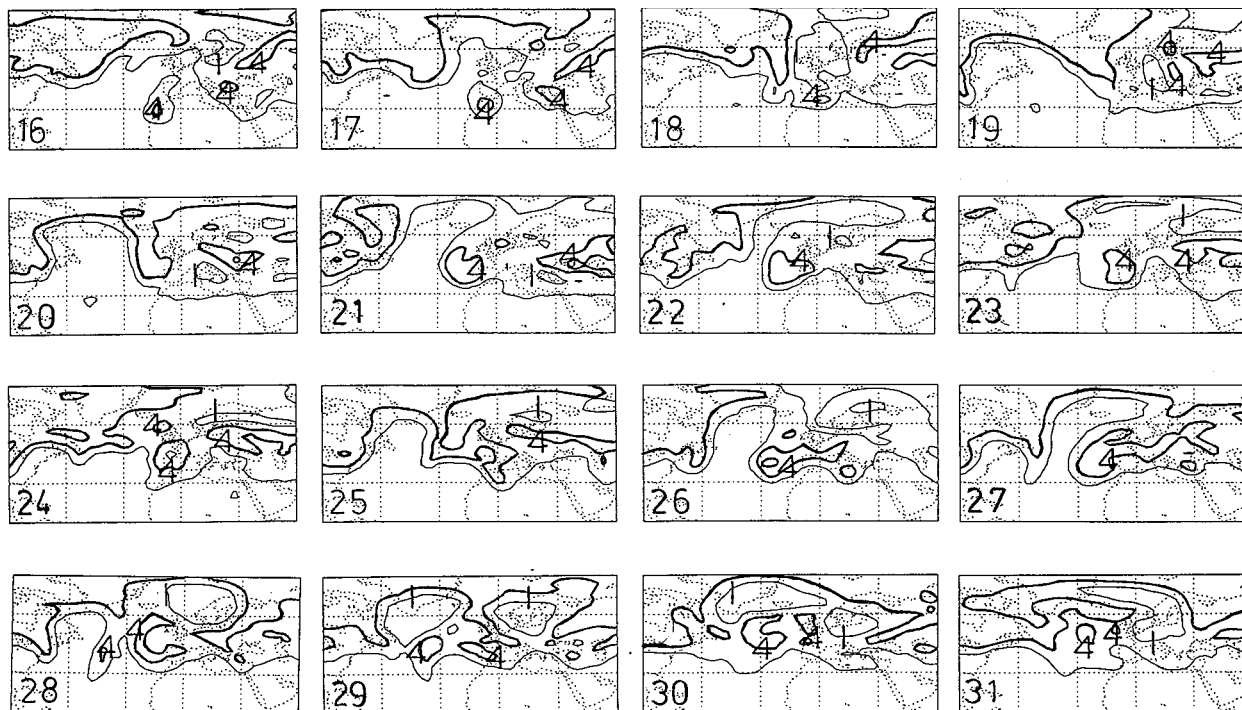
Figure 11. *315 K PV maps for 16–31 January 1996. Only the 1 PVU and 4 PVU contours are shown, with the latter being drawn heavier.*

be absorbed back into the subtropical region downstream of the block.

This PV view of a blocking system emphasises the crucial importance of the upstream weather systems in maintaining it. The picture obtained is amazingly similar to that summarised by Berggren *et al.* (1949). Similar PV maps have been given by Shutts (1986), Hoskins *et al.* (1985) and Hoskins & Sardeshmukh (1987). Theoretical support for the picture has been presented by Shutts (1983) and Vautard & Legras (1988)

6. Further discussion

The PV maps shown in the two case studies have concentrated on a particular level. However, the development on any level is influenced by PV features on other levels, and a more complete description involves them as well. In particular, strong development usually involves interaction with the low level θ distribution. Ahead of a cyclonic PV trough near the tropopause there will be poleward advection of warm air. If a significant warm anomaly at the surface is formed, this too has its associated cyclonic circulation. To the extent that the upper and lower cyclonic anomalies are in phase, then their cyclonic circulations will reinforce. To the extent that the low-level anomaly remains ahead of the upper anomaly, then the associated equatorward flow behind it will act to reinforce the upper PV anomaly. This is the process of 'self-development'.

In the discussion so far it has been assumed that the atmosphere is adiabatic and frictionless and that PV is

consequently materially conserved. For most extratropical synoptic developments this appears to give a good first approximation. In Figures 9 and 11, for example, the extremes were almost conserved. However, the cut-off high and low PV anomalies in the block do gradually decay.

The material change of PV is described in equation (A28). In the free atmosphere the diabatic heating effect can be very important. Above (strictly in the direction of the absolute vorticty vector) a region of latent heat release the PV is decreased and below it the PV is increased. Thus, the latent heating in a mid-latitude low pressure system can lead to significant enhancement of the low level cyclonic circulation, and enhancement of the upper ridge in the air moving ahead of it. A recent detailed analysis of this enhancement in a numerical simulation of an explosive cyclone was given by Stoelinga (1996). The PV increase above a radiative cooling maximum generally occurs at a slower rate than the decrease above a latent heating maximum, and appears to be responsible for the gradual decay of the low PV cut-offs in the blocking anticyclone in Figure 10.

Finally, we note another possible use of PV-θ diagnostics which has yet to be explored fully. A map of a single geopotential contour over many days has been used by F. Sanders and others to summarise the weather in a period, and more recently to summarise an ensemble of forecasts for a certain day (Toft, 1996, pers. commun.). Since a single PV contour on a θ surface (or equivalently, θ on PV) has more dynamical and physical significance it would appear that its use in this
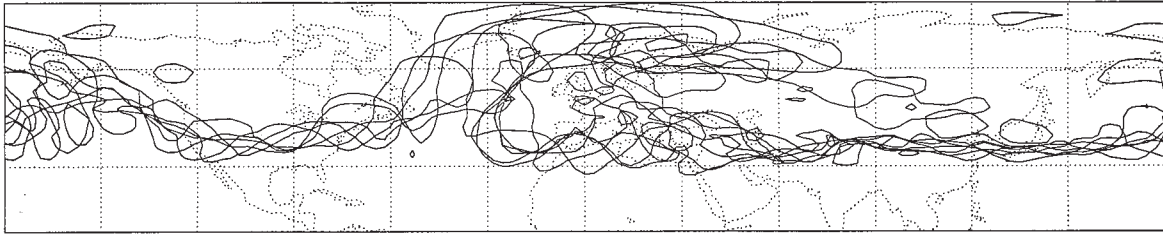
Figure 12. *The 315 K, PV = 2 contour for each day in the week 22–28 January 1996. The region shown is now the whole northern hemisphere between 10° N and 80° N.*

manner would be appropriate. Figure 12 shows such a summary map for the 315 K PV = 2 contour for the week 22–28 January 1996. The different behaviour in different longitudes is readily apparent. There is little variability from 60° E to 180° E, but significant activity in the eastern North Pacific with a tendency to produce transient anticyclonic cut-offs near Alaska. There is a smaller level of wave activity over North America with amplification east of the Great Lakes. Over the North Atlantic the major transient events seen in Figure 11 are evident with the low PV cut-offs tending to drift east–southeast across Asia, while the high PV always extends west–southwest from northern Europe towards the Azores. The Mediterranean region is disturbed through the period.

Acknowledgements

Appendix. Some basic equations in *z*- and *p*-coordinates

A1. Introduction

The equations used here and elsewhere may be considered in the framework of using z or p as vertical coordinate. In this paper they are discussed in the context of z-coordinates, but here we show the equations in both coordinate systems and the transformation from z to p.

A2. The basic equations

The z-coordinate equations with the Boussinesq and incompressible approximations, and the p-coordinate equations are given in Table A1. Throughout $\mathbf{v}$ is the horizontal wind vector $(u, v, 0)$ and ∇_h is the horizontal gradient operator $(\partial/\partial x, \partial/\partial y, 0)$.

The z-coordinate equations may be transformed to the p-coordinate equations by:

$$\phi' = p'/\bar{\rho} \rightarrow \phi', \text{ geopotential deviation}$$

$$z \rightarrow -p$$

$$g/\theta_o \rightarrow (R/p)(p/p_o)^\kappa \equiv \hat{R} \qquad (A5)$$

$$w \rightarrow -\omega$$

$$N^2 = \frac{g}{\theta_o}\frac{d\bar{\theta}}{dz} \rightarrow \sigma^2 = -\hat{R}\frac{d\bar{\theta}}{dp}$$

These substitutions may be made in any of the z-coordinate equations to obtain the corresponding p-coordinate versions.

Table A1. *Basic equations in z- and p-coordinates (the definitions of $\hat{R}$, N^2 and σ^2 are given in equation (A5))*

	z-coordinates	*p*-coordinates	Equations
Variables	$p = \bar{p}(z) + p'$ $\rho = \bar{\rho}(z) + \rho'$ $\theta = \bar{\theta}(z) + \theta'$ $\phi' = p'/\bar{\rho}$ $\theta_0 = typical\ \bar{\theta}$	$\phi = gz$ $\phi = \bar{\phi}(p) + \phi'$ $\theta = \bar{\theta}(p) + \theta'$	
Horizontal momentum equation	$\dfrac{D\mathbf{v}}{Dt} + f\mathbf{k}\times\mathbf{v} + \nabla_h\phi' = \mathbf{0}$	$\dfrac{D\mathbf{v}}{Dt} + f\mathbf{k}\times\mathbf{v} + \nabla_h\phi' = \mathbf{0}$	(A1/z), (A1/p)
Hydrostatic equation	$\dfrac{\partial\phi'}{\partial z} = \dfrac{g}{\theta_o}\theta'$	$\dfrac{\partial\phi'}{\partial p} = \hat{R}\theta'$	(A2/z), (A2/p)
Continuity equation	$\nabla_h\cdot\mathbf{v} + \dfrac{\partial w}{\partial z} = 0$	$\nabla_h\cdot\mathbf{v} + \dfrac{\partial\omega}{\partial p} = 0$	(A3/z), (A3/p)
Thermodynamic equation	$\dfrac{D}{Dt}\dfrac{g\theta'}{\theta_o} + N^2 w = 0$	$\dfrac{D\hat{R}\theta'}{Dt} - \sigma^2\omega = 0$	(A4/z), (A4/p)

A3. Derived equations in *z*-coordinates

(a) Vector vorticity equation

The absolute vorticity is:

$$\zeta = f\mathbf{k} + \nabla \times \mathbf{v}$$

where ∇ is the three-dimensional gradient operator:

$$\left(\frac{\partial}{\partial x}, \frac{\partial}{\partial y}, \frac{\partial}{\partial z} \right).$$

Therefore:

$$\zeta = \left(-\frac{\partial v}{\partial z}, \frac{\partial u}{\partial z}, f + \frac{\partial v}{\partial x} - \frac{\partial u}{\partial y} \right). \qquad \text{(A6/z)}$$

The vector vorticity equation is:

$$\frac{D\zeta}{Dt} = (\zeta \cdot \nabla)\,\mathbf{u} - \mathbf{k} \times \nabla \frac{g}{\theta_o} \theta'. \qquad \text{(A7/z)}$$

where $\mathbf{u}$ is the three-dimensional wind vector (u,v,w).

The vertical component of absolute vorticity is $\zeta = f + \xi$ where the relative vorticity is given by:

$$\xi = \frac{\partial v}{\partial x} - \frac{\partial u}{\partial y}.$$

The vertical component of the vorticity equation is:

$$\frac{D}{Dt}(f + \xi) = -\frac{\partial v}{\partial z}\frac{\partial w}{\partial x} + \frac{\partial u}{\partial z}\frac{\partial w}{\partial y} + (f + \xi)\frac{\partial w}{\partial z}. \qquad \text{(A8/z)}$$

(b) Geostrophic motion

The geostrophic velocity is:

$$\mathbf{v}_g = (u_g, v_g) = \left(-\frac{\partial \psi}{\partial y}, \frac{\partial \psi}{\partial x} \right). \qquad \text{(A9)}$$

where the geostrophic streamfunction $\psi = \phi'/f_0$. Then the geostrophic relative vorticity is:

$$\xi_g = \frac{\partial v_g}{\partial x} - \frac{\partial u_g}{\partial y} = \frac{\partial^2 \psi}{\partial x^2} + \frac{\partial^2 \psi}{\partial y^2} = \nabla_h^2 \psi \qquad \text{(A10)}$$

and:

$$\frac{g}{\theta_o} \theta' = f_o \frac{\partial \psi}{\partial z}. \qquad \text{(A11/z)}$$

The thermal wind equations are:

$$f_o \frac{\partial u_g}{\partial z} = -\frac{g}{\theta_o}\frac{\partial \theta'}{\partial y}$$
$$\hspace{6cm} \text{(A12/z)}$$
$$f_o \frac{\partial v_g}{\partial z} = \frac{g}{\theta_o}\frac{\partial \theta'}{\partial x}$$

$$f_o \frac{\partial \xi_g}{\partial z} = \frac{g}{\theta_o} \nabla_h^2 \theta'. \qquad \text{(A13/z)}$$

The rate of change following the geostrophic wind is:

$$D_g = \frac{\partial}{\partial t} + \mathbf{v}_g \cdot \nabla_h. \qquad \text{(A14)}$$

(c) Quasi-geostrophic (QG) equations

With the QG approximation the vertical component of the vorticity equation (equation (A8/z)) becomes:

$$D_g(f + \xi_g) = f_o \frac{\partial w}{\partial z}. \qquad \text{(A15/z)}$$

The QG thermodynamic equation (equation (A4/z)) is:

$$D_g \frac{g}{\theta_o} \theta' = -N^2 w. \qquad \text{(A16/z)}$$

Eliminating w between equations (A15/z) and (A16/z) gives:

$$D_g q = 0 \qquad \text{(A17)}$$

where the QG Potential Vorticity (QGPV) is:

$$q = f + \xi_g + f_o \frac{\partial}{\partial z}\left(\frac{g}{\theta_o} \theta' / N^2 \right). \qquad \text{(A18/z)}$$

In terms of the geostrophic streamfunction the QGPV becomes:

$$q = f + \frac{\partial^2 \psi}{\partial x^2} + \frac{\partial^2 \psi}{\partial y^2} + \frac{\partial}{\partial z}\left(\frac{f_o^2}{N^2} \frac{\partial \psi}{\partial z} \right). \qquad \text{(A19/z)}$$

Alternatively, using thermal wind balance (equations (A12/z) or (A13/z)), the time derivative can be eliminated between equations (A15/z) and (A16/z) to give a diagnostic equation for vertical velocity:

$$N^2 \nabla_h^2 w + f_o^2 \frac{\partial^2 w}{\partial z^2} = F. \qquad \text{(A20/z)}$$

This is referred to as the omega equation.

Using $\partial/\partial t$ of equation (A12/z) for the elimination gives:

$$F = f_o \frac{\partial}{\partial z}(\mathbf{v}_g \cdot \nabla_h \xi_g)$$
$$-\nabla_h^2\left(\mathbf{v}_g \cdot \nabla_h \frac{g}{\theta_o} \theta' \right) + f_o \beta \frac{\partial v_g}{\partial z}. \qquad \text{(A21/z)}$$

This is the vorticity advection, thermal advection (VATA) form for F. In equation (A21/z), θ' may be replaced by θ, and θ'/θ_0 can be replaced by T/T_0.

The Sutcliffe approximation is to neglect the β term and a term that depends on the rotation with height of the axis of deformation (the dilatation axis):

$$F \simeq F_s = 2B \frac{\partial \xi_g}{\partial s} \qquad (A22)$$

where:

$$B = \left| f_o \frac{\partial \mathbf{v}_g}{\partial z} \right| = \left| \nabla_h \frac{g}{\theta_o} \theta' \right| \qquad (A23/z)$$

and s is measured along a θ contour in the direction of the thermal wind.

A full form for F, analogous to equation (A22) but equivalent to equation (A21/z,) is the $\mathbf{Q}$-vector form

$$F = 2\nabla_h \cdot \mathbf{Q} + f_o \beta \frac{\partial v_g}{\partial z} \qquad (A24/z)$$

where

$$\mathbf{Q} = -B \mathbf{k} \times \frac{\partial \mathbf{v}_g}{\partial s} . \qquad (A25)$$

(d) Potential vorticity

The full potential vorticity, often associated with the names Rossby and Ertel, is obtained by combining the vector vorticity equation (A7/z) and the thermodynamic energy equation (A4/z) to give:

$$\frac{DP}{Dt} = 0 \qquad (A26)$$

where the potential vorticity (PV) is given by:

$$P = \frac{1}{\rho} \zeta \cdot \nabla \theta . \qquad (A27/z)$$

In the presence of diabatic heating $\dot\theta$ and momentum source $\mathbf{F}$:

$$\frac{DP}{Dt} = \frac{1}{\rho} \zeta \cdot \nabla \dot\theta + \frac{1}{\rho} (\nabla \times \mathbf{F}) \cdot \nabla \theta . \qquad (A28)$$

A3. Derived equations in p-coordinates

All the equations in section A2 in z-coordinates may be transformed by equation (A5) to give their corresponding p-coordinate form. Here only some of these will be displayed.

In p-coordinates the hydrostatic and thermal wind relations can be written in terms of the geostrophic streamfunction and vorticity:

$$\hat{R}\theta' = -f_o \frac{\partial \psi}{\partial p} \qquad (A11/p)$$

Potential vorticity view of synoptic development

$$-f_o \frac{\partial \xi_g}{\partial p} = \hat{R} \nabla_h^2 \theta' . \qquad (A13/p)$$

The QG vorticity and thermodynamic equatons are:

$$D_g (f + \xi_g) = f_o \frac{\partial \omega}{\partial p} \qquad (A15/p)$$

$$D_g \hat{R}\theta' = + \sigma^2 \omega . \qquad (A16/p)$$

Moving with the geostrophic wind there is conservation of QGPV:

$$q = f + \xi_g - f_o \frac{\partial}{\partial p} \left(\hat{R}\theta' \big/ \sigma^2 \right) . \qquad (A18/p)$$

In terms of the geostrophic streamfunction the QGPV becomes:

$$q = f + \frac{\partial^2 \psi}{\partial x^2} + \frac{\partial^2 \psi}{\partial y^2} + \frac{\partial}{\partial p} \left(\frac{f_o^2}{\sigma^2} \frac{\partial \psi}{\partial p} \right) . \qquad (A19/p)$$

The omega equation is:

$$\sigma^2 \nabla_h^2 \omega + f_o^2 \frac{\partial^2 \omega}{\partial p^2} = -F \qquad (A20/p)$$

where:

$$-F = + f_o \frac{\partial}{\partial p} \left(\mathbf{v}_g \cdot \nabla_h \xi_g \right) + \nabla_h^2 \left(\mathbf{v}_g \cdot \nabla_h \hat{R}\theta' \right)$$

$$+ f_o \beta \frac{\partial v_g}{\partial p} . \qquad (A21/p)$$

The Sutcliffe approximation to F takes the same form as equation (A22) with:

$$B = \left| f_o \frac{\partial \mathbf{v}_g}{\partial p} \right| = \left| \nabla_h \hat{R}\theta' \right| . \qquad (A23/p)$$

The full $\mathbf{Q}$-vector form is:

$$F = 2\nabla_h \cdot \mathbf{Q} - f_o \beta \frac{\partial v_g}{\partial p} \qquad (A24/p)$$

where $\mathbf{Q}$ is defined as in equation (A25).

In an adiabatic, frictionless atmosphere and not making the QG approximation, the full PV:

$$P = -\frac{1}{g} \zeta \cdot \nabla \theta \qquad (A27/p)$$

is conserved following the fluid. Diabatic and frictional changes in PV are again given by equation (A28).

References

Berggren, R., Bolin, B. & Rossby, C. G. (1949). An aerological study of zonal motion, its perturbations and breakdown. *Tellus*, **1**: 14–37.

Hoskins, B. J. (1991). Towards a PV-θ view of the general circulation. *Tellus*, **43AB:** 27–35.

Hoskins, B. J. & Berrisford, P. (1988). A potential vorticity perspective on the storm of 15–16 October 1987. *Weather*, **43:** 122–129.

Hoskins, B. J. & Sardeshmukh, P. D. (1987). A diagnostic study of the dynamics of the northern hemisphere winter of 1985/86. *Q. J .R. Meteorol. Soc.,* **113:** 759–778.

Hoskins, B. J., McIntyre, M. E. & Robertson, A. W. (1985). On the use and significance of isentropic potential vorticity maps. *Q. J. R. Meteorol. Soc.,* **111:** 877–946.

Pedder, M. A. (1997). The omega equation: Q-G interpretations of simple circulation features. *Meterol. Appl.,* **4:** 335–344.

Shutts, G. J. (1983). The propagation of eddies in diffluent jet-streams: eddy vorticity forcing of 'blocking' flow fields. *Q. J. R. Meteorol. Soc.,* **109:** 737–761.

Shutts, G. J. (1986). A case study of eddy forcing during an Atlantic blocking episode. *Adv. Geophys.,* **29:** 135–162.

Stoelinga, M. (1996). A potential vorticity-based study of the role of diabatic heating and friction in a numerically simulated cyclone. *Mon. Wea. Rev.,* **124:** 849–874.

Thorpe, A. J. (1985). Diagnosis of balanced vortex structure using potential vorticity. *J. Atmos. Sci.,* **42:** 397–406.

Vautard, R. & Legras, B. (1988). On the source of mid-latitude low frequency variability. Part II: Nonlinear equilibration of weather regimes. *J. Atmos. Sci.,* **45:** 2845–2867.